Low-Resistance Ferromagnetic Tunnel Junction

●Hideyuki Kikuchi   ●Masashige Sato   ●Kazuo Kobayashi
(Manuscript received September 7, 2001)

To develop the next-generation magnetic read head, we investigated ferromagnetic tunnel junctions (MTJs) with a low resistance and a high magneto-resistance (MR) ratio, the MTJs were fabricated by Ultra High Vacuum (UHV) magnetron sputtering with various Al layer thicknesses and oxidization conditions. The MR ratio dependencies on the RS (junction resistance × area) values were studied.

By optimizing the barrier thickness and oxidization conditions, we fabricated an MTJ with a 0.9 nm Al-O barrier layer that has an MR ratio of 20% and an RS of 7.8 $\Omega\mu m^2$. When the thickness of the Al-O barrier layer in the MTJ was less than 0.9 nm, RS was below about 10 $\Omega\mu m^2$. However, the MR ratio and the breakdown voltage decreased when RS was decreased. We found that the decreases in MR ratio and the breakdown processes at a low RS were caused by pinholes in the barrier layer. Therefore, to obtain an MTJ with a low RS and a high MR ratio for the next-generation magnetic read head, we will optimize the deposition conditions and find materials for making a thinner barrier layer without pinholes.

1. Introduction

The capacity of magnetic disk systems is growing year by year. Recently, the use of the spin-valve (SV) reading head has increased the areal-density growth rate to higher than 100%. As a result, the current areal density in commercial HDDs is about 30 Gbit/in² and the reading heads of these HDDs have an MR ratio of about 10%. Further, the areal density of HDDs is certain to exceed 100 Gbit/in² in the next few years. However, because of the extremely small size of the recording areas at these densities, it will then be very difficult to increase the MR ratio of an SV head so that it is sensitive enough to read the recorded information.

Since 1995, when Takahashi demonstrated a ferromagnetic tunnel junction (MTJ) with a ferromagnetic metal-insulator-ferromagnetic metal structure that had an MR ratio of 18% at room temperature,[1] it has been common knowledge that MTJs have a larger MR ratio than SV films, which makes them a candidate for the reading heads of future HDDs.[2)-4)] **Figure 1** shows a schematic diagram of an MTJ head.

In 1996, we were the first research group to find an annealing effect that increased the MR ratio of the MTJ to over 25%.[5] Then, in 1999 we demonstrated an MTJ with an MR ratio of over 40% that was fabricated using $CoFe_{26}$ ferromagnetic layers and an annealing process.[6] However, MTJs with a 40% MR ratio have a large RS of more than 1k $\Omega\mu m^2$, which will cause significant problems in terms of the reading data rate and head noise.

The reading data rate is limited by the reading head resistance R and the capacitance C between the reading head and the reading driver IC, because these two components combine to form a low-pass filter.[7] The cut-off frequency fc of this
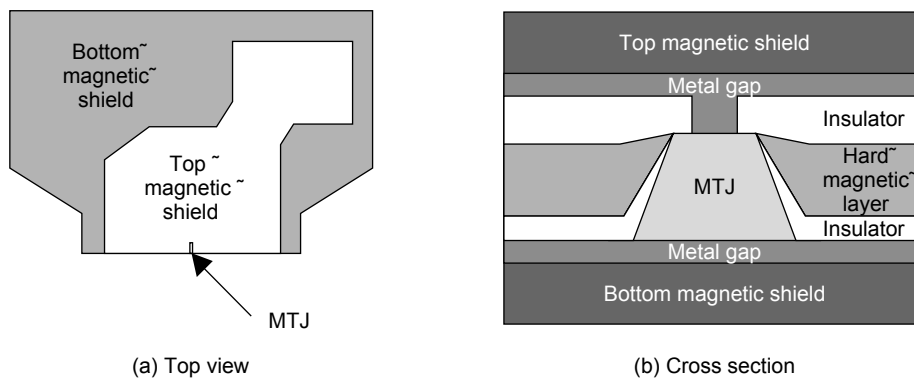
(a) Top view

(b) Cross section

Figure 1
MTJ reading head.

low-pass filter is given by:

$$fc = 1/(2\pi RC)$$

The reading head resistance should be about 100 Ω when fc is 1 GHz and C is in the pF region. Therefore, RS must be less than 10 Ωμm².

On the other hand, the head noise consists of the Johnson noise caused by thermal activity and the shot noise caused by voltage fluctuations. The shot noise voltage v is given by:

$$v^2 = 2eVR_eB_w$$

where e is the electron charge, V is the bias voltage, R_e is the element resistance, and B_w is the bandwidth. The shot noise voltage shows a linear dependency on the bias voltage and is greater than the Johnson noise voltage. Therefore, R_e must be low to reduce the noise.

For these reasons, the reading data rate and noise considerations dictate that reading heads for recording densities over 100 Gbit/in² must have an RS of less than 4 Ωμm² to compete with the present SV heads.

Therefore, we investigated MTJs with a low RS and a high MR ratio. In this paper, we describe several MTJs with a low RS and investigate their electrical properties.

2. Experiment

The MTJs we investigated had a seed layer and 4 nm of NiFe, 3 nm of $CoFe_{26}$, 0.9 to 1.2 nm of Al-AlO, 2.5 nm of $CoFe_{26}$, 15 nm of IrMn, and 20 nm of Au on a 5-inch silicon wafer with a 1 μm thermally oxidized surface. Each layer was deposited using a UHV magnetron sputtering system with a base pressure below 3×10^{-7} Pa. Ultra-clean Ar and O_2 gases were used for the deposition and oxidization, respectively. The Al layer was oxidized immediately after the Al layer was deposited with the natural oxidization method. After depositing the Al layer, the ultra-clean O_2 gas was introduced to the chamber at 100 sccm to increase the O_2 pressure in the chamber at the rate of 100 Pa/min. When the O_2 pressure reached the oxidization pressure, the O_2 gas supply was stopped and the oxidation pressure was maintained throughout the oxidization period.

MTJ elements from 0.033 to 900 μm² were patterned with photolithography. **Figure 2** shows the schematic diagram of the MTJ and the MTJ's structure.

The four-probe method was used for measuring the resistances, MR properties, and resistance-voltage (R-V) characteristics. A magnetic field was applied in the same direction as that of the magnetization in the pinned layer (CoFe under IrMn layer). All measurements were made at room temperature. The barrier height and the barrier width of the oxidized Al layer were calculated by fitting the measured R-V characteristics to Simons' equation.[8]
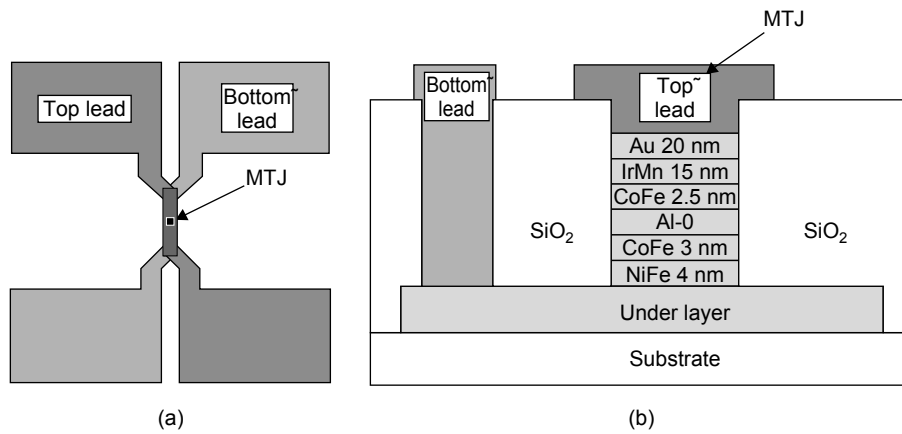
184

FUJITSU Sci. Tech. J.,**37**, 2,(December 2001)

Figure 2
Schematic diagram of the MTJ and its layer structure.
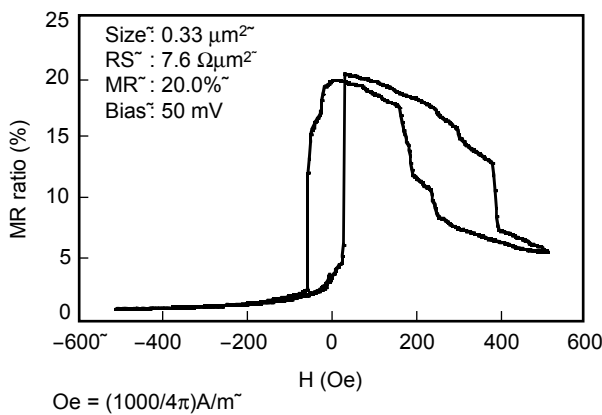
Figure 3
MR curve of low-resistance MTJ.

Figure 4
Dependence of barrier properties on Al thickness and oxidization pressure.

3. Results and discussions

3.1 Dependence of barrier height and width on Al layer thickness

Figure 3 shows a typical MR curve of a low-resistance MTJ. A spin-valve-like R-H property is observed. When a large magnetic field is applied, the tunnel resistance is low because the magnetization of the NiFe/CoFe bottom layer and CoFe top layer are parallel (P). On the other hand, when a low magnetic field is applied, the tunnel resistance is high because the magnetization of the NiFe/CoFe bottom layer is switched and becomes antiparallel (AP) with that of the CoFe top layer.

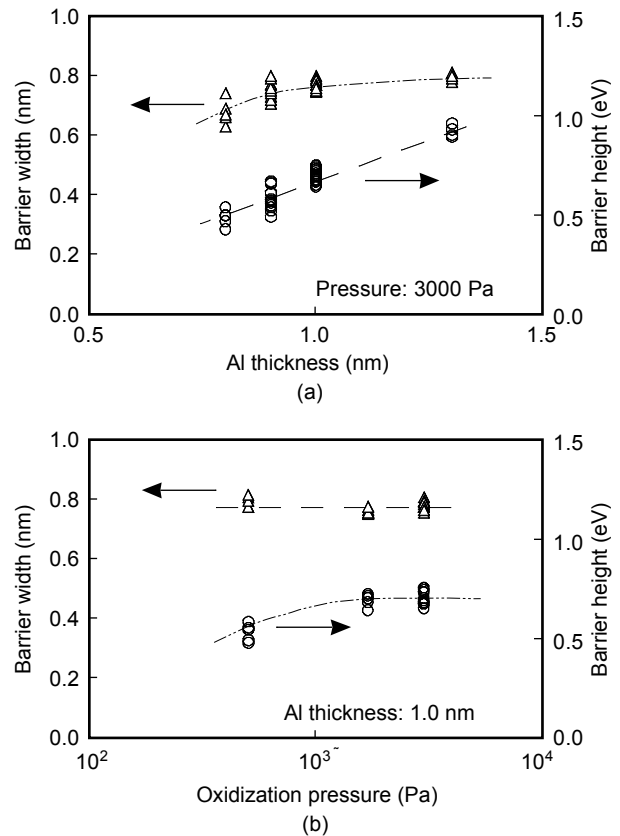The shape of the R-H curve is not good due to the presence of a magnetic domain structure in the MTJ. This magnetic domain structure occurs because the MTJ area is very small and does not have a hard magnetic layer for magnetic domain control. **Figure 4 (a)** shows the dependence of the barrier height and the barrier width on the Al

layer thickness. The oxidization times were 30 minutes at 3000 Pa O_2. The barrier width increases with the Al thickness and becomes constant at 0.8 nm at Al thicknesses of 1.0 nm and above.

Figure 4 (b) shows the dependence of the barrier height and barrier width on the O_2 gas pressure. The oxidization time was 30 minutes at each O_2 pressure. When the O_2 pressure is low, the barrier height also becomes low. We found that the barrier height and barrier width are influenced by the Al layer thickness and oxidization conditions. We should therefore pay attention to the fact that the barrier height and barrier width cannot be accurately estimated from Simons' equation, because the equation assumes a rectangular barrier potential but the actual shape of the barrier potential is not rectangular.[8),9)] Therefore, in this paper we restrict ourselves to a relatively qualitative discussion of the barrier thickness and height.

3.2 Dependence of MR ratio on RS

Figure 5 (a) shows the dependence of the MR ratio on the RS values of MTJs deposited by the UHV sputtering system and the conventional sputtering system (base pressure $< 1 \times 10^{-4}$ Pa) fabricated with different Al thicknesses, O_2 pressures, and oxidization times. The MTJs deposited with the UHV sputtering system show an MR ratio of over 20% and an RS that is two orders of magnitude lower than that of the MTJs deposited by the conventional sputtering system.

In **Figure 5 (b)**, which shows a closeup of the 10 $\Omega\mu m^2$ area in Figure 5 (a), we can see that the MR ratios of the MTJs deposited by UHV sputtering stay constant at about 20% when RS is over 10 $\Omega\mu m^2$, but begin to drop when RS goes below 10 $\Omega\mu m^2$.

Most of the MTJs with a low RS have a thin Al-O layer. The MR ratios of MTJs deposited using the conventional sputtering system decreased monotonically with RS, and MTJs with an RS of 200 $\Omega\mu m^2$ and a 1.3 nm Al-O thickness had an

MR ratio of less than 5%.

On the other hand, the MR ratios of the UHV-sputtered MTJs were not significantly reduced even when the RS was reduced to 10 $\Omega\mu m^2$ (0.9 nm Al-O thickness).

These results show that the UHV sputtering system can make a thinner Al-O barrier layer than the conventional sputtering system. This suggests that the difference between these sputtering systems occurs because the UHV sputtering system makes layers that are purer, more uniform, and have a smoother interface than the conventional system, because of the UHV back-pressure and the ultra-clean gas.

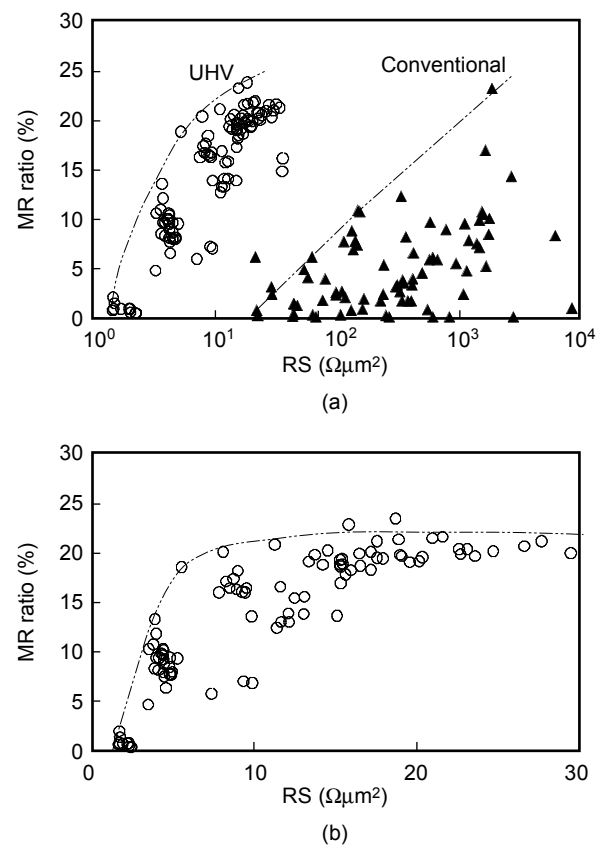Therefore, the deposition conditions must be optimized to obtain an MTJ with a low RS and a high MR ratio.

(a)

(b)

Figure 5
Dependence of MR ratio on RS values in MTJs fabricated with various Al thicknesses, O_2 pressures, and oxidization times.

3.3 Breakdown processes

Figure 6 shows the breakdown processes when voltage was applied to samples with (a) a high RS value (> 100 $\Omega\mu m^2$) and (b) a low RS value (< 11 $\Omega\mu m^2$). The MTJs were 1 μm^2. One of two kinds of breakdown processes occurs, depending on the RS value.

When the RS is high, it decreases gradually according to the tunnel property as the applied voltage is increased. Then, when the voltage exceeds 0.95 V, the RS suddenly falls at a point called the breakdown voltage (V_b). This suggests that the barrier layer is eventually broken down and pinholes start to appear. Assuming that the barrier thickness is 0.8 nm as estimated from Figure 4, the electric field caused by the breakdown voltage is of the order of 10^{-9} V/m. The reasons for the breakdown that occurs when this electric field is applied are explained using the E model, which assumes that Al^{3+} ions break through the barrier layer, and the 1/E model, which assumes that electrons trapped in defects and impurities break through the barrier layer.[10],[11]

When the RS is low, the resistance gradually decreases as the applied voltage is increased up to about 0.35 V (V_b). Then, between about 0.35 V and 0.4 V, the resistance falls off dramatically. These decreases in resistance in the high-RS and low-RS MTJs occur for different reasons. When the RS is low, there are many pinholes in the barrier layer, which offer a current path that is parallel with the tunnel path. The localized heating caused by the increased applied voltage gradually increases the size of these pinholes. As a result, the resistance of the pinholes decreases and the RS also decreases.

Figure 7 shows the dependence of V_b on the RS. The MTJ size is 1 μm^2. The MTJs with a high RS have a high V_b, and V_b decreases with a decreasing RS. Especially, there is a remarkable decrease in V_b when RS is about 20 $\Omega\mu m^2$. The breakdown process of MTJs with a high RS corresponds to Figure 6 (a), and the breakdown process of MTJs with a low RS corresponds to Figure 6 (b). Therefore, an MTJ with an RS below 20 $\Omega\mu m^2$ seems to have pinholes in the barrier layer.
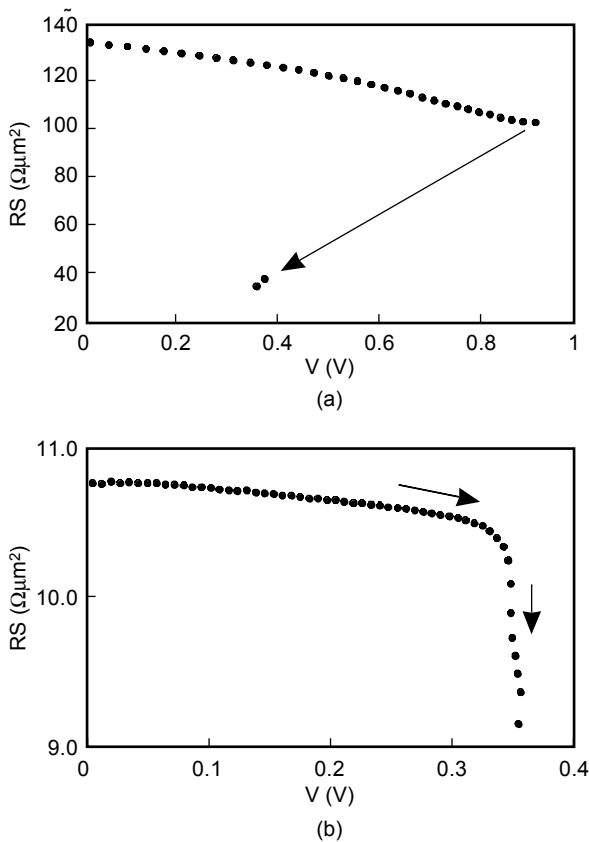

Figure 6
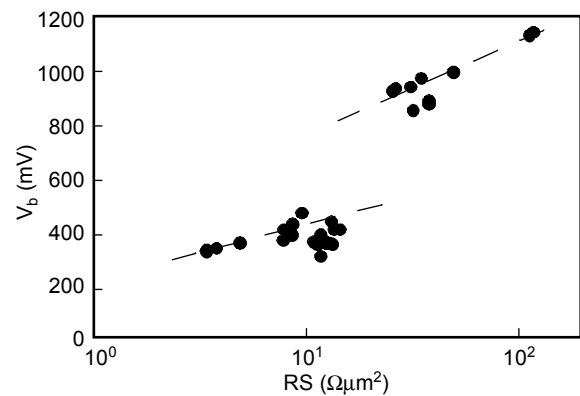Breakdown processes in samples with (a) a high RS value and (b) a low RS value.

Figure 7
Dependence of breakdown voltage on RS.

Figure 8 shows the dependence of V_b on the MTJ area, S. The RS values of these MTJs are about 25 $\Omega\mu m^2$. The figure shows that V_b depends on S, which indicates the existence of pinholes in the barrier layer. When S is large, the probability of pinholes occurring in the barrier layer becomes high and the V_b decreases. Also, even if an MTJ

has a low V_b, V_b might be improved by making the MTJ smaller.

Figure 9 (a) shows how the MR ratio changes with RS as an MTJ is destroyed by increasing V_b. Each MR ratio and RS value was obtained immediately after the new V_b was applied, and the process was repeated until the MR ratio became 0%. As the figure shows, the MR ratio falls as RS is reduced. The slopes of the data lines are indicated by the dashed lines and depend on the Al thickness, d_{Al}.

Figure 9 (b) shows the normalized MR ratio dependence on the bias voltage before and after the breakdown voltage is applied. The normalized bias voltage dependence does not change after the breakdown.

Therefore, the initial TMR characteristics remain after breakdown by V_b.

Figure 10 shows the R-V curves (a) before and (b) after breakdown. The curves in Figure 9 (a) are
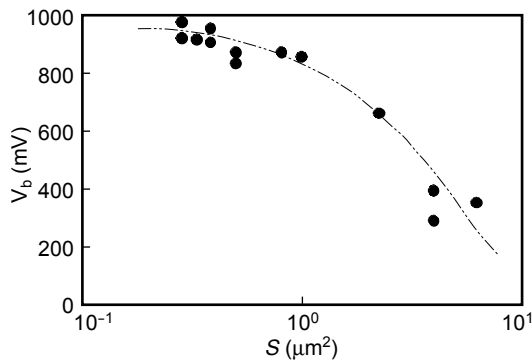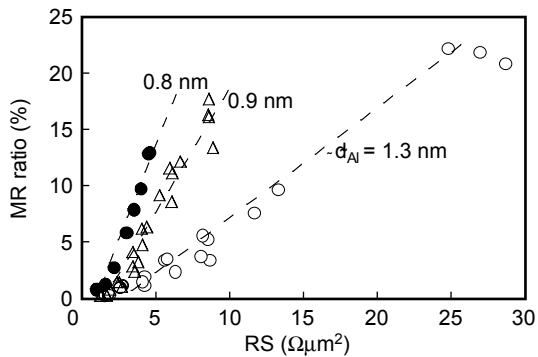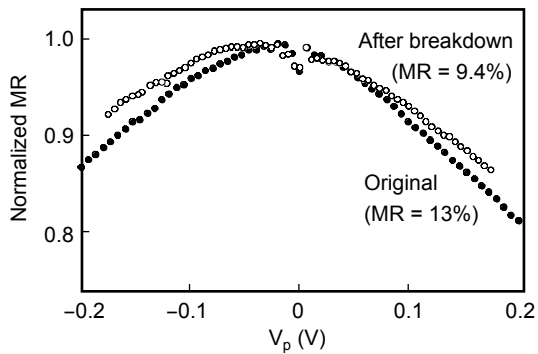

Figure 8
Dependence of breakdown voltage on element area.

(a) Relationship between RS and MR ratio

(b) Bias dependences before and after breakdown

Figure 9
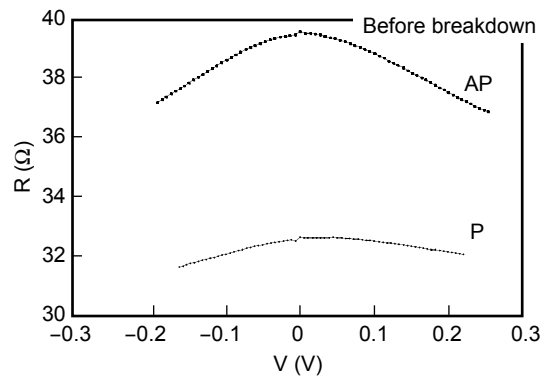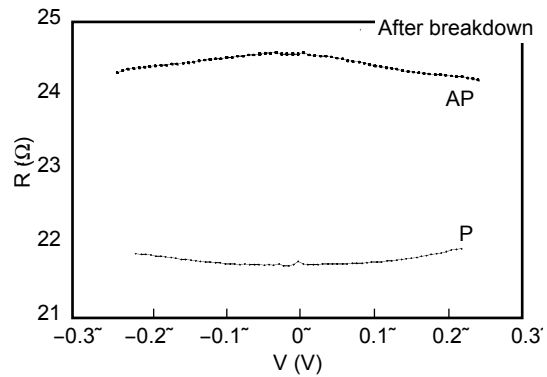Properties during breakdown process.

(a) Before breakdown

(b) After breakdown

Figure 10
R-V curves.

inverse parabolas, which suggests that the current through the MTJ is mostly tunnel current. On the other hand, when the magnetization of the NiFe/CoFe bottom layer and CoFe top layer are parallel (P), the curves in Figure 9 (b) are parabolic, which suggests that the current through the MTJ is mostly leakage current. Nevertheless, the MTJ in Figure 9 (b) still has an MR ratio.

The results in Figures 8 to 10 show that there are both destroyed and undamaged areas in the barrier layer after breakdown. Therefore, the current after breakdown consists of leakage current through pinholes in the breakdown areas and tunnel current that flows through the undamaged areas.

3.4 Calculated properties of MTJ circuit for this assumption

To investigate the MTJ property with the pinholes in the barrier layer, we assumed that there is a resistance caused by pinholes that is in parallel with the tunnel resistance. **Figure 11** shows the equivalent electrical circuit.

The mean resistance of the MTJ (R_{meas}) is given by:

$$R_{meas} = (R_T \times R_P)/(R_T + R_P)$$
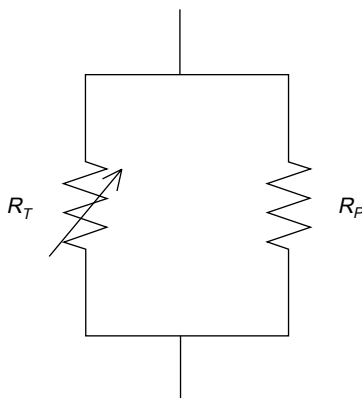
where R_T is the tunnel resistance and R_P is the

pinhole resistance. The applied magnetic field changes R_T but not R_P. R_T and ΔR_T, which is the difference in R_T between the AP and P states of the applied magnetic field, do not depend on R_P.

Figure 12 shows the calculated properties. Figure 12 (a) shows that R_{maes} decreases as

(a)

(b)

(c)

Figure 12
Calculated properties of element with pinholes.
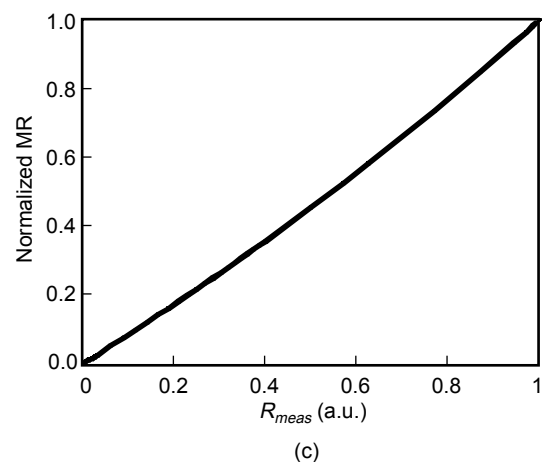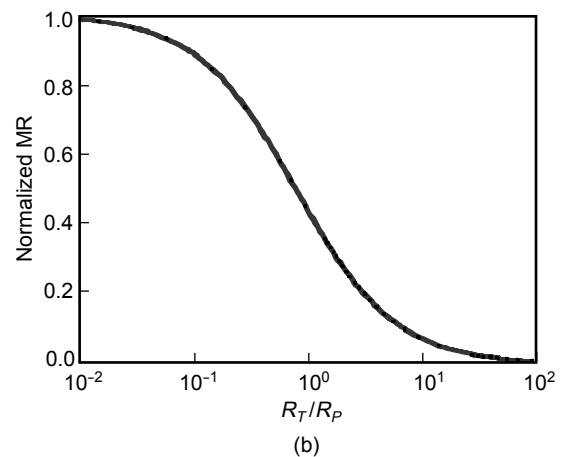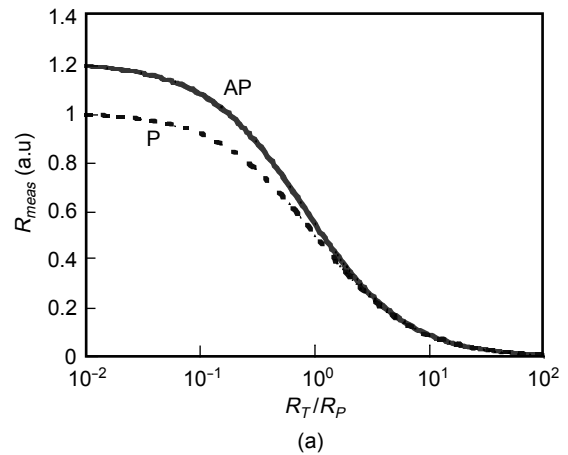

Figure 11
Equivalent electrical circuit for calculating properties of element with pinholes.

R_T/R_P is increased. In this case, the MR ratio is the difference in R_{meas} between the AP and P states and decreases as R_T/R_P is increased. Figure 12 (b) shows the MR ratio versus R_T/R_P. The MR ratio decreases when R_T/R_P is increased; therefore, the relation between the normalized MR ratio and R_{maes} is as shown in Figure 12 (c). This calculated data agrees well with the experiment data for the low-resistance MTJs whose properties are shown in Figure 9 (a). Therefore, we can conclude that there are many pinholes in the barrier layer and that the MR ratio decreases when the resistance of the MTJs is low.

4. Conclusion

1) By optimizing the deposition conditions and Al thickness, we fabricated an MTJ with an MR ratio of 20% and an RS of 7.8 $\Omega\mu m^2$. However, the MR ratio decreases with the RS when the RS is less than about 10 $\Omega\mu m^2$. We need to determine the optimal deposition conditions and oxidization method for obtaining an MTJ with a higher MR ratio and a lower RS.

2) The breakdown processes differ between MTJs with a high RS and MTJs with a low RS. MTJs with a low RS break down easily. Breakdown in MTJs with a high RS occurs because of the electric field, and breakdown in MTJs with a low RS occurs because of the heating caused by current through pinholes.

3) The leakage current makes the RS and the MR ratio small. The relation between the RS and MR ratio becomes directly proportional when the RS is low or the MTJ is broken down by the applied voltage. This suggests that this directly proportional relationship is caused by the pinholes.

We found that MTJs with a low RS show a low MR ratio due to the leakage current through pinholes in the barrier layer. The breakdown voltage in an MTJ with an RS of 10 $\Omega\mu m^2$ is about 300 to 400 mV. The breakdown voltage can be slightly improved by making the MTJ small. How-ever, a higher breakdown voltage is required in a reading head. To make an MTJ with a lower RS, higher MR ratio, and higher breakdown voltage, we need to make a thinner barrier layer without pinholes. To achieve this, we will optimize the deposition conditions and find an underlayer material that provides an automatically smooth surface. We must do more work to obtain an MTJ with a lower resistance and a higher MR ratio; for example, we need to investigate other barrier layer materials and develop new structures.

Recently, the existence of pinhole in the barrier layer was investigated by the measurement of low temperature dependent resistance of MTJ[12]. We will start that measurement. And, MTJ heads that use a high-RS MTJ have been reported by other research groups that are investigating the properties of MTJ heads.[13],[14] We also will make an MTJ head and measure its properties as soon as possible.

5. References

1) T. Miyazaki and N. Tesuka: Spin polarization tunneling in ferromagnet/insulator/ferromagnet junctions. *J. Magn. Magn. Mater.*, **151**, p.403 (1995).

2) K. Shimazawa, O. Redon, N. Kasahara, J. J. Sun, K. Sato, T. Kagami, S. Saruki, T. Umehara, Y. Fujita, S. Yarimizu, S. Araki, H. Morita, and M. Matsuzaki: Evaluation of Front Flux Guide-Type Magnetic Tunnel Junction Heads. *IEEE Trans. Magn.*, **36**, p.2542-2544 (2000).

3) D. Song, J. Nowak, R. Larson, P. Kolbo, and R. Chellew: Demonstrating a Tunneling Magneto-Resistive Read Head. *IEEE Trans. Magn.*, **36**, p.2545-2548 (2000).

4) K. Ohashi, K. Hayashi, K. Nagahara, K. Ishihara, E. Fukami, J. Fujikita, S. Mori, M. Nakada, T. Mitsuzuka, K. Matsuda, H. Mori, A. Kamijo, and H. Tsuge: Low-Resistance Tunnel Magnetoresistive Head. *IEEE Trans. Magn.*, **36**, p.2549-2553 (2000).

5) M. Sato and K. Kobayashi: Spin-Valve-Like

Properties and Annealing Effect in Ferromagnetic Tunnel Junctions. *IEEE Trans. Magn.*, **33**, p.3553 (1997).

6) H. Kikuchi, M. Sato, and K. Kobayashi: Effect of CoFe Composition of the Spin-valve-Like Ferromagnetic Tunnel Junction. *J. Appl. Phys.*, **87**, p.6055-6057 (2000).

7) K. Kobayashi: The Object of Tunnel Giant Magnetoresistance. (in Japanese), *Monthly Electronics Magazine*, **9**, p.35-37 (1998).

8) J. G. Simmons: Electric Tunnel Effect between Dissimilar Electrodes Separated by a Thin Insulating Film. *J. Appl. Phys.*, **34**, p.2581-2590 (1963).

9) B. J. Jönsson-Akerman, R. Escudero, C. Leighton, S. Kim, Ivan K. Schuller, and D. A. Rabson: Reliability of normal-state current-voltage characteristics as an indicator of tunnel-junction barrier quality. *Appl. Phys. Lett.*, **77**, p.1870-1872 (2000).

10) Y. Ando, H. Kameda, H. Kubota, and T. Miyazaki: Local Transport Property on Ferromagnetic Tunnel Junction Measured Using Conducting Atomic Force Microscope. *Jpn.* *J. Appl. Phys.*, **38**, p.L737-L739 (1999).

11) W. Oepts, H. J. Verhagen, W. J. M. de Jonge, and R. Coehoorn: Dielectric breakdown of ferromagnetic tunnel junctions. *Appl. Phys. Lett.*, **73**, p.2363-2365 (1998).

12) U. Rüdiger, R. Calaro, U. May, K. Samm, J. Hauch, H. Kittur, M. Sperlich, and G. Güntherodt: Temperature Dependent Resistance of Magnetic Tunnel Junctions As A Quality Proof of The Barrier. *J. Appl. Phys.*, **89**, p.7573-7575(2001).

13) K. Shimazawa, J. J. Sun, N. Kasahara, K. Sato, T. Kagami, S. Sakurai, O. Redon, Y. Fujita, T. Umehara, J. Syoji, A. Araki, and M. Matsuzaki: Frequency Response of Common Lead and Shield Type Magenetic Tunneling Junction Head. *IEEE Trans. Magn.*, **37**, p.1684-1686 (2001).

14) K. Ishihara, M. Nakada, E. Fukami, K. Nagahara, H. Honjo, and K. Ohashi: Read Performance of Tunneling Magnetoresistive Heads. *IEEE Trans. Magn.*, **37**, p.1687-1690 (2001).

Hideyuki Kikuchi received the B.E. and M.E. degrees in Electrical Engineering from Nihon University, Tokyo, Japan in 1988 and 1990, respectively.
He joined Fujitsu Laboratories Ltd., Atsugi, Japan in 1990, where he has been engaged in research of materials for the magnetic heads of hard disk drives. He is a member of the Magnetics Society of Japan and the Physical Society of Japan.

Kazuo Kobayashi received the B.S., M.E, and Dr. degrees from Tohoku University, Sendai, Japan in 1968, 1970, and 1995, respectively. He joined Fujitsu Laboratories Ltd., Kawasaki, Japan in 1970, where he has been engaged in research of materials and devices for the magnetic heads and media of hard disk drives. He is a member of the Magnetics Society of Japan, the Physical Society of Japan, and the Applied Physical Society of Japan.

Masashige Sato received the B.E. and M.E. degrees in Applied Physics from Tohoku University, Sendai, Japan in 1992 and 1994, respectively. He joined Fujitsu Laboratories Ltd., Atsugi, Japan in 1994, where he has been engaged in research of materials for the magnetic heads of hard disk drives. He is a member of the Magnetics Society of Japan.

FUJITSU Sci. Tech. J.,**37**, 2,(December 2001)

191